

Decomposition Methods and Strain Driven Algorithms for Limit and Shakedown Analysis

Giovanni Garcea and Leonardo Leonetti

Abstract A mathematical programming formulation of strain-driven path-following strategies to perform shakedown and limit analysis for perfectly elastoplastic materials in a FEM context, is presented. From the optimization point of view, standard arc-length strain driven elastoplastic analysis, recently extended to shakedown, are identified as particular decomposition strategies used to solve a proximal point algorithm applied to the static shakedown theorem that is then solved by means of a convergent sequence of safe states. The mathematical programming approach allows: a direct comparison with other nonlinear programming methods, simpler convergence proofs and duality to be exploited. Due to the unified approach in terms of total stresses, the strain driven algorithms become more effective and less nonlinear with respect to a self equilibrated stress formulation and easier to implement in existing codes performing elastoplastic analysis.

1 Introduction

The static and kinematic shakedown theorems, including the limit analysis as a special case, furnish, in a direct and elegant fashion, a reliable safety factor against plastic collapse, loss in functionality due to excessive deformation (ratcheting) or collapse due to low cycle fatigue (plastic shakedown) [1]. Based on these theorems the so called *direct methods* evaluate the safety factor solving a nonlinear convex optimization problem that usually involves hundreds of thousands of unknowns and constraints when real structures are discretized by means of finite elements.

Nowadays this kind of problems could be efficiently solved using interior point methods (IPM) especially when the problem is formulated as a conic programming one and the solution is obtained using primal dual formulations. The work done in this field is impressive and in rapid development: significant references can be

G. Garcea (✉) · L. Leonetti

Dipartimento di Modellistica per l'Ingegneria, Università della Calabria, Rende, Italy
e-mail: giovanni.garcea@unical.it

L. Leonetti

e-mail: leonetti.leonardo@gmail.com

found in the works of Boyd [5], Bertsekas [7], Nemirosky and Todd [8] and Wright [6, 9] among others. As a great number of yield constraints are described as second order cones efficient interior point algorithms for shakedown and limit analysis have been proposed (see [11–17] and references therein). Alternatively the limit load can also be obtained by means of the complete reconstruction of the elasto-plastic equilibrium path, using standard path-following strain driven strategies (see Armero [2] for a review). An extension of these consolidated and widely used algorithms for shakedown analysis was proposed in [3, 4].

In this work it will be show how strain driven elastoplastic analysis based on closest point projection return mapping schemes and Riks arc-length solution, can be obtained from a mathematical programming problem, consisting in the application of the proximal point algorithm to the static shakedown theorem and in the solution of this problem by means of dual decomposition methods [7, 18, 19]. In particular the pseudo elasto-plastic step coincides with a step of the proximal point algorithm (see also [10] for a similar formulation) while the optimization subproblems, deriving from the decomposition techniques, correspond exactly to the standard return mapping by closest point projection scheme used to evaluate the plastically admissible stress.

To obtain a unified formulation for limit and shakedown analysis, the problem is formulated in terms of global stress and equivalent reference load. This choice is particularly advantageous in the strain driven case because it allows a less nonlinear formulation of the problem and makes it easy to fulfill some convergence requirements of the algorithm. The proposed formulation is similar to that presented in [3] and, due to the requirement, in the shakedown case, of a Multi-Surface Return Mapping process, will be called *MS-RM*. The mathematical programming point of view also enables the formulation of a new decomposition strategy based on a Single Surface Return Mapping which will be called *SS-RM*. It requires the solution of the same closest point projection problem as in the standard limit analysis case.

Apart from the mathematical programming reformulation, strain driven incremental analysis due to its classical mechanical interpretation, gives other important information in addition to the shakedown or limit load multiplier evaluation. For the fixed load case, the extremal paths theory of Ponter and Martin [20], gives a coherent justification for the holonomic transformation of the incremental constitutive elasto-plastic relationships obtained by means of a backward Euler integration scheme (closest point return mapping algorithm) and a mechanical sense to the so evaluated equilibrium path allowing the reuse of the static and kinematic parts of the solution at each equilibrium point. A similar interpretation also holds for shakedown where the solution algorithm can be viewed as a step-by-step incremental process aiming to simulate the case of a proportional increase in the domain of the loads such that, for each new point of the equilibrium path, the load recycles within all admissible combinations, up to the achievement of elastic adaptation. This interpretation also allows a possible extension of the strain driven algorithms to the shakedown analysis of more complex materials.

Strain driven algorithms are compared, in terms of performance, accuracy and robustness with the solution obtained with the commercial code MOSEK [24] im-

plementing an Interior Point solution method. The application regards plane stress problems with von Mises yield functions.

The work is organized as follows: in Sect. 2 shakedown theory is presented and rewritten in a discrete FEM form for simpler use in a mathematical programming context; in Sect. 3 shakedown theorems and a mathematical programming version of the elastoplastic step and its relation with proximal point methods is presented; in Sect. 4 we illustrate the numerical methods used to evaluate the shakedown load; in Sect. 5 we give some details on the numerical implementations of the algorithms proposed; in Sect. 6 the finite element discretization is presented; finally in Sect. 7 an extensive series of numerical tests showing the reliability and effectiveness of the proposed formulation is reported.

2 The Discrete Equation for Shakedown and Limit Analysis

In the following, limit and shakedown problems are reformulated in terms of finite element algebraic equations for a better framing in the usual mathematical programming notation.

2.1 The Discrete Representation of Static and Kinematic Fields

Using a mixed finite element format and a vector notation, we assume that the displacement $\mathbf{d}[\mathbf{x}] \in \mathfrak{N}^{n_u}$ and the stress $\boldsymbol{\sigma}[\mathbf{x}] \in \mathfrak{N}^{n_\sigma}$ of a point \mathbf{x} of the body domain \mathcal{B} are interpolated as:

$$\boldsymbol{\sigma}[\mathbf{x}] = \mathbf{N}_\sigma[\mathbf{x}]\mathbf{t}, \quad \mathbf{d}[\mathbf{x}] = \mathbf{N}_u[\mathbf{x}]\mathbf{u} \quad (1)$$

where $\mathbf{N}_\sigma[\mathbf{x}]$ and $\mathbf{N}_u[\mathbf{x}]$ collect the interpolation functions while global vectors \mathbf{u} and \mathbf{t} collect the N_σ stress node vectors $\boldsymbol{\sigma}_g := \boldsymbol{\sigma}[\mathbf{x}_g]$ and N_u displacement node vectors $\mathbf{d}_i := \mathbf{d}[\mathbf{x}_i]$ in a finite numbers of points as:

$$\mathbf{t} = \begin{bmatrix} \boldsymbol{\sigma}_1 \\ \vdots \\ \boldsymbol{\sigma}_{N_\sigma} \end{bmatrix}, \quad \mathbf{u} = \begin{bmatrix} \mathbf{d}_1 \\ \vdots \\ \mathbf{d}_{N_u} \end{bmatrix}$$

Making $\mathbf{D}[\mathbf{x}]$ the kinematical operator, the relationship between strain $\boldsymbol{\varepsilon}[\mathbf{x}] \in \mathfrak{N}^{n_\sigma}$ and displacements $\mathbf{d}[\mathbf{x}]$ can be written as:

$$\boldsymbol{\varepsilon}[\mathbf{x}] = \mathbf{N}_\varepsilon[\mathbf{x}]\mathbf{d}, \quad \mathbf{N}_\varepsilon = \mathbf{D}[\mathbf{x}]\mathbf{N}_u[\mathbf{x}]$$

Using the virtual work expression, the finite element representation of the equilibrium equations becomes:

$$\mathbf{Q}^T \mathbf{t} = \lambda \mathbf{p} \quad \text{with} \quad \mathbf{Q}^T \equiv \int_B \mathbf{N}_\varepsilon[\mathbf{x}]^T \mathbf{N}_\sigma[\mathbf{x}] dV \quad (2)$$

and the external force vector, when only mechanical actions are considered, is

$$\mathbf{p} = \int_{\mathcal{B}} \mathbf{N}_u^T \mathbf{b}[\mathbf{x}] dV + \int_{\partial_f \mathcal{B}} \mathbf{N}_u^T \mathbf{f}[\mathbf{x}] dA$$

$\mathbf{b}[\mathbf{x}]$ being the external body forces and $\mathbf{f}[\mathbf{x}]$ the surface force on the boundary $\partial_f \mathcal{B}$. The discrete form of the compatibility condition is

$$\boldsymbol{\rho} = \mathbf{Q} \mathbf{u} \quad (3)$$

where $\boldsymbol{\rho} = [\boldsymbol{\varepsilon}_1, \dots, \boldsymbol{\varepsilon}_{N_\sigma}]^T$ collects the discrete strain conjugate, in the virtual work sense, to \mathbf{t} . Finally linear elastic constitutive law is defined by the elastic operator $\mathbf{E}[\mathbf{x}]$ so that

$$\boldsymbol{\sigma}[\mathbf{x}] = \mathbf{E}[\mathbf{x}] \boldsymbol{\varepsilon}[\mathbf{x}], \quad \boldsymbol{\varepsilon}[\mathbf{x}] = \mathbf{E}[\mathbf{x}]^{-1} \boldsymbol{\sigma}[\mathbf{x}] \quad (4)$$

From now on the dependence of quantities on \mathbf{x} will be omitted for an easier reading.

2.2 The Elastic Envelope of the Stresses

We assume that the external actions \mathbf{p} are expressed as a combination of basic loads \mathbf{p}_i belonging to the admissible closed and convex *load domain*

$$\mathbb{P} := \left\{ \mathbf{p} \equiv \sum_{i=1}^p a_i \mathbf{p}_i : a_i^{\min} \leq a_i \leq a_i^{\max} \right\} \quad (5)$$

Denoting with \mathbf{t}_{ei} the elastic stress solution for \mathbf{p}_i , the *elastic envelope* \mathbb{S}_e

$$\mathbb{S}_e := \left\{ \mathbf{t}_e \equiv \sum_{i=1}^p a_i \mathbf{t}_{ei} : a_i^{\min} \leq a_i \leq a_i^{\max} \right\} \quad (6)$$

defines the set of the elastic stresses \mathbf{t}_e produced by each load path contained in \mathbb{P} .

By construction \mathbb{S}_e and \mathbb{P} are convex polytopes and each $\mathbf{t}_e \in \mathbb{S}_e$ can be expressed as a convex combination of the N_v elastic envelope vertexes $\mathbf{t}^{E\alpha}$ that can be usefully referred to the reference stress \mathbf{t}^{E0} so obtaining:

$$\mathbf{t}_e = \mathbf{t}^{E0} + \sum_{\alpha=1}^{N_v} t^\alpha \mathbf{t}^{E\alpha}, \quad t^\alpha \geq 0, \quad \sum_{\alpha=1}^{N_v} t^\alpha = 1 \quad (7)$$

If the external loads increase by a real number λ the elastic envelope becomes $\lambda \mathbb{S}_e := \{\lambda \mathbf{t}_e : \mathbf{t}_e \in \mathbb{S}_e\}$.

Note that the vertexes of the stress envelope could be a subset of the 2^p vertexes of \mathbb{P} , however, to simplify the presentation we assume, from now on, $N_v = 2^p$.

2.3 The Shakedown Elastic Domain

Assuming elastic perfectly plastic material the stress σ will be *plastically admissible* if

$$f[\sigma[\mathbf{x}]] \equiv \phi[\sigma[\mathbf{x}]] - \sigma_y[\mathbf{x}] \leq 0 \quad \forall \mathbf{x} \in \mathcal{B} \quad (8)$$

where the yield function f is a sum of the homogeneous convex function ϕ and of the yield stress $\sigma_y \in \mathbb{R}$. In a FEM context of analysis the previous condition could be expressed in a weighted sense on the element, as proposed for example in [22], or tested in a finite number of points. For the sake of simplicity we assume control of plastic admissibility in the N_σ stress nodes so that \mathbf{t} will be plastically admissible if

$$\mathbf{f}[\mathbf{t}] \leq \mathbf{0} \iff f[\sigma_g] \leq 0 \quad \forall g = 1, \dots, N_\sigma \quad (9)$$

where, from now on, vector inequality will be considered in a componentwise fashion and

$$\mathbf{f}[\mathbf{t}] = [f[\sigma_1] \ f[\sigma_2] \ \dots \ f[\sigma_{N_\sigma}]]^T, \quad f[\sigma_g] \equiv \phi[\sigma_g] - \sigma_{gy} \quad (10)$$

with $\sigma_{gy} := \sigma_y[\mathbf{x}_g]$.

Finally it is useful to express the plastically admissible condition for all the stresses contained in the amplified elastic envelope $\lambda \mathbb{S}_e$ translated by $\tilde{\mathbf{t}}$. Due to the convexity of \mathbf{f} and \mathbb{S}_e this can be easily expressed in terms of the plastic admissibility of all vertex stresses $\mathbf{t}^\alpha = \lambda(\mathbf{t}^{E\alpha} + \mathbf{t}^{E0}) + \tilde{\mathbf{t}}$

$$\mathbf{f}[\lambda \mathbf{t}_e + \tilde{\mathbf{t}}] \leq \mathbf{0}, \quad \forall \mathbf{t}_e \in \mathbb{S}_e \iff \mathbf{f}[\mathbf{t}^\alpha] \leq \mathbf{0}, \quad \forall \alpha \quad (11)$$

From now on we denote with a Greek superscript vertex quantities.

3 Shakedown and Limit Analysis Multipliers

Shakedown theorems used for the evaluation of the larger multiplier λ_a , called *shakedown safety factor*, amplifying the load domain \mathbb{P} are rewritten in a unified format. A particular mathematical programming technique, the proximal point algorithm, to solve the static shakedown theorem will also be introduced. We always refer to shakedown analysis, the limit analysis case being simply obtained when the elastic envelope collapses in a single point.

3.1 Shakedown Theorems

Sufficient and necessary conditions for shakedown are given in the classic shakedown theorems [1] that will be written in a form suitable for FEM numerical implementations. In particular the Bleich–Melan static theorem is formulated in terms of

total stress, instead of self-equilibrated ones, making a unified notation for shake-down and limit analysis possible. The Koiter kinematical theorem is obtained as the dual, from the optimization point of view, of the primal static theorem so as to ensure an easy extension, to these discrete forms, of a series of properties regarding existence, uniqueness, duality gap, etc.

3.1.1 Static Theorem, Safe Multipliers and Multipliers Bounds

The static theorem states that a load domain multiplier λ_s will be safe if there exists a time-independent self-equilibrated stress field $\bar{\mathbf{t}}$ so that each stress in $\lambda_s \mathbb{S}_e + \{\bar{\mathbf{t}}\}$ is plastically admissible. The multiplier λ_a can be evaluated as the maximum of these safe multipliers recasting the static theorems in terms of the reference stress \mathbf{t}^{E0} :

$$\begin{aligned} & \text{maximize} \quad \lambda_s \\ & \text{subject to} \quad \mathbf{Q}^T \mathbf{t} = \lambda_s \mathbf{p} \\ & \quad \mathbf{t}^\alpha = \mathbf{t} + \lambda_s \mathbf{t}^{E\alpha}, \quad \alpha = 1, \dots, N_v \\ & \quad \mathbf{f}[\mathbf{t}^\alpha] \leq \mathbf{0}, \quad \alpha = 1, \dots, N_v \end{aligned} \tag{12a}$$

with $\mathbf{p} \equiv \mathbf{Q}^T \mathbf{t}^{E0}$ and $\mathbf{t} \equiv \bar{\mathbf{t}} + \lambda_s \mathbf{t}^{E0}$. When $\mathbf{t}^{E0} = \mathbf{0}$ we have the classic form in terms of the self-equilibrated stress. Furthermore, without any loss in generality, we can set \mathbf{t}^{E0} as a generic vertex of \mathbb{S}_e so \mathbf{t} becomes the total stress of this vertex. We assume $\mathbf{t}^{E1} \equiv \mathbf{0}$ so deleting in (12a) the constraint $\mathbf{t} \equiv \mathbf{t}^1$. An equivalent formulation for (12a) is obtained eliminating all the variables \mathbf{t}^α using the linear equality constraints and so the admissible conditions become:

$$\mathbf{f}^\alpha[\mathbf{t}, \lambda] \equiv \mathbf{f}[\mathbf{t} + \lambda \mathbf{t}^{E\alpha}] \leq \mathbf{0}. \tag{12b}$$

When the external load domain collapses in a single point ($a_i^{\min} = a_i^{\max}$) Eqs. (12a) directly transform into the standard form of the static theorem of limit analysis. From (12a) we have that λ_a will be no greater than the values of the limit load multiplier obtained for a generic $\mathbf{p} \in \mathbb{P}$, and then also of the limit load of each vertex of \mathbb{P} . It is worth noting that the *plastic shakedown multiplier* $\bar{\lambda}$, simply obtained by deleting the equilibrium constraints in Eq. (12a), is not less than λ_a . Its evaluation, as will be better shown in the sequel, is obtained by solving a series of small optimization subproblems.

Finally Eq. (12a) can be rewritten, using a compact notation, in a format similar to that of the static theorem of the limit analysis:

$$\begin{aligned} & \text{maximize} \quad \lambda_s \\ & \text{subject to} \quad \tilde{\mathbf{Q}}^T \tilde{\mathbf{t}} = \lambda_s \tilde{\mathbf{p}} \\ & \quad \tilde{\mathbf{f}}[\tilde{\mathbf{t}}] \leq \mathbf{0} \end{aligned} \tag{12c}$$

where the following quantities have been defined

$$\tilde{\mathbf{t}} := \begin{bmatrix} \mathbf{t}^1 \\ \vdots \\ \mathbf{t}^{N_v} \end{bmatrix}, \quad \tilde{\mathbf{f}}[\tilde{\mathbf{t}}] := \begin{bmatrix} \mathbf{f}[\mathbf{t}^1] \\ \vdots \\ \mathbf{f}[\mathbf{t}^{N_v}] \end{bmatrix}, \quad \tilde{\mathbf{p}} := \begin{bmatrix} \mathbf{p} \\ \mathbf{t}^E \end{bmatrix}, \quad \mathbf{t}^E := \begin{bmatrix} \mathbf{t}^{E2} \\ \vdots \\ \mathbf{t}^{EN_v} \end{bmatrix} \quad (13)$$

and

$$\tilde{\mathbf{Q}}^T := \begin{bmatrix} \mathbf{Q}^T & \cdot \\ -\boldsymbol{\Sigma}^T & \mathbf{I}_\alpha \end{bmatrix}, \quad \boldsymbol{\Sigma} := -[\mathbf{I} \quad \cdots \quad \mathbf{I}] \quad (14)$$

where \cdot , \mathbf{I} and \mathbf{I}_α are respectively zero and identity matrices of the appropriate dimension. From now on we denote with a Greek superscript the vertex components of a (\cdot) vector or matrix. The superscript 1, that denotes quantities of the reference vertex, will be omitted when inessential.

3.1.2 The Dual Problem: The Kinematical Theorem

Static theorem is a primal nonlinear convex optimization problem. The Lagrangian associated to it is

$$\mathcal{L}[\lambda, \tilde{\mathbf{t}}, \tilde{\boldsymbol{\mu}}, \Delta \tilde{\mathbf{u}}] = \lambda + \Delta \tilde{\mathbf{u}}^T (\tilde{\mathbf{Q}}^T \tilde{\mathbf{t}} - \lambda \tilde{\mathbf{p}}) - \tilde{\boldsymbol{\mu}}^T \tilde{\mathbf{f}}[\tilde{\mathbf{t}}]$$

where the Lagrange multipliers assume the following expression

$$\tilde{\boldsymbol{\mu}} := \begin{bmatrix} \boldsymbol{\mu}^1 \\ \vdots \\ \boldsymbol{\mu}^{N_v} \end{bmatrix}, \quad \boldsymbol{\mu}^\alpha := \begin{bmatrix} \mu_1^\alpha \\ \vdots \\ \mu_{N_\sigma}^\alpha \end{bmatrix}, \quad \tilde{\mathbf{u}} := \begin{bmatrix} \Delta \mathbf{u} \\ \Delta \boldsymbol{\rho} \end{bmatrix}, \quad \Delta \boldsymbol{\rho} := \begin{bmatrix} \Delta \boldsymbol{\rho}^2 \\ \vdots \\ \Delta \boldsymbol{\rho}^{N_v} \end{bmatrix}$$

with each $\boldsymbol{\mu}^\alpha \geq \mathbf{0}$. In the optimal values the Lagrangian has a saddle point [5, 7] making it possible to obtain the following dual problem that, with simple algebra, becomes the discrete form of the Koiter kinematical theorem:

$$\begin{aligned} &\text{minimize} \quad \lambda_c \equiv \tilde{\boldsymbol{\sigma}}_y^T \tilde{\boldsymbol{\mu}} \\ &\text{subject to} \quad \tilde{\boldsymbol{\mu}} \geq \mathbf{0} \\ &\quad \quad \quad \tilde{\mathbf{u}}^T \tilde{\mathbf{p}} = 1 \\ &\quad \quad \quad \tilde{\mathbf{Q}} \tilde{\mathbf{u}} - \tilde{\mathbf{A}}[\tilde{\mathbf{t}}] \tilde{\boldsymbol{\mu}} = \mathbf{0} \end{aligned} \quad (15a)$$

where $\tilde{\boldsymbol{\sigma}}_y$ collect the yield stress values

$$\tilde{\boldsymbol{\sigma}}_y = \begin{bmatrix} \boldsymbol{\sigma}_y \\ \vdots \\ \boldsymbol{\sigma}_y \end{bmatrix}, \quad \boldsymbol{\sigma}_y = \begin{bmatrix} \sigma_{y1} \\ \vdots \\ \sigma_{yN_\sigma} \end{bmatrix}$$

and

$$\tilde{\mathbf{A}}[\tilde{\mathbf{t}}] := \left(\frac{\partial \mathbf{f}[\tilde{\mathbf{t}}]}{\partial \tilde{\mathbf{t}}} \right)^T = \text{blockdiag} [\mathbf{A}^1 \dots \mathbf{A}^{N_v}] \quad (15b)$$

$\mathbf{A}^\alpha = \left(\frac{\partial \mathbf{f}[\mathbf{t}^\alpha]}{\partial \mathbf{t}^\alpha} \right)^T$ being a diagonal matrix.

In the previous equations the Euler theorem for the homogeneous functions of order one has been used while the extension to homogeneous functions of order n is simple. Also for kinematical theorem (15a) we have the same format as the limit analysis case.

The saddle point property of the Lagrangian shows that the primal problem is convex and the dual is concave. When the first one has an admissible solution, that is when the elastic limit multiplier is other than zero, both problems have the same optimal value $\lambda_a = \max \lambda_s = \min \lambda_c$. Due to the convexity of the problem the obtained optimum is global such that the shakedown (limit) load factor is unique.

3.2 The Mathematical Programming Formulation of the Finite Step Elasto-plastic Analysis

The shakedown multipliers can also be obtained by evaluating a sequence of states, $\mathbf{z}^{(k)} := \{\lambda^{(k)}, \mathbf{t}^{(k)}, \mathbf{u}^{(k)}, \dots\}$ solving a series of problems so defined:

$$\begin{aligned} & \text{maximize} \quad \Delta \xi^{(k)} \lambda^{(k)} - \frac{1}{2} \Delta \tilde{\mathbf{t}}^T \tilde{\mathbf{F}} \Delta \tilde{\mathbf{t}} \\ & \text{subject to} \quad \tilde{\mathbf{Q}}^T \tilde{\mathbf{t}}^{(k)} = \lambda^{(k)} \tilde{\mathbf{p}} \\ & \quad \quad \quad \tilde{\mathbf{f}}[\tilde{\mathbf{t}}^{(k)}] \leq \mathbf{0} \end{aligned} \quad (16a)$$

where the superscript $(\cdot)^{(k)}$ will denote quantities evaluated in the k th of problems (16a) called the k th step, the symbol $\Delta(\cdot) = (\cdot)^{(k)} - (\cdot)^{(k-1)}$ is the increment of a quantity from the previous step and $\Delta \xi^{(k)} > 0$ is a real positive number. In the block-diagonal semi-definite positive matrix $\tilde{\mathbf{F}} := \text{blockdiag}[\mathbf{F}^1 \dots \mathbf{F}^{N_v}]$ only \mathbf{F}^1 must be definite positive and can be evaluated through the following energy equivalence

$$\mathbf{F}^1 \equiv \mathbf{F} = \int_B \mathbf{N}_\sigma[\mathbf{x}]^T \mathbf{E}^{-1}[\mathbf{x}] \mathbf{N}_\sigma[\mathbf{x}] dV \quad (16b)$$

Note that, due to the local nature of the stress interpolation in Eq. (1), \mathbf{F} also has a block diagonal structure that, usually, couples only the local finite element stress variables. In the following we assume, to simplify the notation and according to the finite element used, each block \mathbf{F}_g^α of \mathbf{F}^α to be defined at the stress node level.

Table 1 First order conditions for the proximal point algorithm

<i>Local level:</i>		
Kinem. compatib.:	$\begin{cases} \mathbf{Q}\Delta\mathbf{u} - \sum_{\beta=2}^{N_v} \Delta\rho^\beta - \mathbf{F}\Delta\mathbf{t}^1 - \mathbf{A}^1\boldsymbol{\mu}^1 = 0 \\ \Delta\rho^\beta = \mathbf{F}^\beta\Delta\mathbf{t}^\beta + \mathbf{A}^{\beta(k)}\boldsymbol{\mu}^{\beta(k)} \end{cases}$	$\beta := 2 \cdots N_v$
Yielding:	$\mathbf{f}[\mathbf{t}^{\alpha(k)}] \leq \mathbf{0}$	$\alpha := 1 \cdots N_v$
Consistency:	$(\boldsymbol{\mu}^{\alpha(k)})^T \mathbf{f}[\mathbf{t}^{\alpha(k)}] = 0$	$\alpha := 1 \cdots N_v$
Dual feasibility	$\boldsymbol{\mu}^{\alpha(k)} \geq \mathbf{0}$	$\alpha := 1 \cdots N_v$
Elastic domain:	$\mathbf{t}^{\alpha(k)} = \mathbf{t}^{(k)} + \lambda^{(k)} \mathbf{t}^{E\alpha}$	$\alpha := 1 \cdots N_v$
<i>Global level:</i>		
Equilibrium:	$\mathbf{Q}^T \mathbf{t}^{(k)} = \lambda^{(k)} \mathbf{p}_0$	
Normalization:	$\Delta\mathbf{u}^T \mathbf{p} + \sum_{\beta=2}^{N_v} (\Delta\rho^\beta)^T \mathbf{t}^{E\beta} = \Delta\xi^{(k)}$	

The first order Kunh–Tucker conditions of (16a) are:

$$\begin{aligned}
\text{Kinematical compat.:} \quad & \tilde{\mathbf{Q}}\Delta\tilde{\mathbf{u}} = \tilde{\mathbf{F}}\Delta\tilde{\mathbf{t}} + \tilde{\mathbf{A}}^{(k)}\tilde{\boldsymbol{\mu}}^{(k)} \\
\text{Yielding:} \quad & \tilde{\mathbf{f}}[\tilde{\mathbf{t}}^{(k)}] \leq \mathbf{0} \\
\text{Consistency:} \quad & \tilde{\mathbf{f}}[\tilde{\mathbf{t}}^{(k)}]^T \tilde{\boldsymbol{\mu}}^{(k)} = 0 \\
\text{Dual feasibility} \quad & \tilde{\boldsymbol{\mu}}^{(k)} \geq \mathbf{0} \\
\text{Extended equilibrium:} \quad & \tilde{\mathbf{Q}}^T \tilde{\mathbf{t}}^{(k)} - \lambda^{(k)} \tilde{\mathbf{p}} = \mathbf{0} \\
\text{Arc-length constraint:} \quad & \tilde{\mathbf{p}}^T \Delta\tilde{\mathbf{u}} = \Delta\xi^{(k)}
\end{aligned} \tag{16c}$$

which are also explicitly reported in Table 1. Equations (16c), for $\tilde{\mathbf{F}}\Delta\tilde{\mathbf{t}} = \mathbf{0}$, apart from the inessential scaling for $\Delta\xi^{(k)}$, are the primal–dual conditions of the shakedown theorems. Problem (16a) is similar to that presented in [10].

Note as, for assigned values of \mathbf{u} and λ , the first group of equations in Table 1, due to the block structures of \mathbf{f} and \mathbf{F} , can be solved at the *local level* (stress node) of the analysis. Conversely, equilibrium equations and normalization condition, coupling all the variables of the problem, define the *global level* of the analysis.

3.2.1 Convergence Properties of the Sequence of Elasto-plastic Steps

Starting from the known elastic limit $\mathbf{z}^{(0)}$, the sequence $\mathbf{z}^{(k)}$ generated from successive solutions of Eq. (16a) is safe in the sense of the static theorem and monotonously increasing in $\lambda^{(k)}$. In fact, due to Eq. (16c), subtracting the equilibrium equation of the two steps (k) and $(k-1)$ and multiplying the results by $\Delta\tilde{\mathbf{u}}$ we have

$$\Delta\lambda\Delta\xi^{(k)} = \Delta\tilde{\mathbf{t}}^T \tilde{\mathbf{Q}} \Delta\tilde{\mathbf{u}}$$

where the condition $\Delta\tilde{\mathbf{u}}^T \tilde{\mathbf{p}} = \Delta\xi^{(k)}$ was used. Due to the kinematical compatibility equations, we obtain

$$\begin{aligned} \Delta\xi^{(k)} \Delta\lambda &= \Delta\tilde{\mathbf{t}}^T \tilde{\mathbf{F}} \Delta\tilde{\mathbf{t}} + \Delta\tilde{\mathbf{t}}^T \tilde{\mathbf{A}}^{(k)} \tilde{\boldsymbol{\mu}}^{(k)} \\ &= \underbrace{\Delta\tilde{\mathbf{t}}^T \tilde{\mathbf{F}} \Delta\tilde{\mathbf{t}}}_{\geq 0} + \sum_{\alpha=1}^{N_v} \underbrace{(\Delta\tilde{\mathbf{t}}^\alpha)^T \mathbf{A}^{\alpha(k)} \boldsymbol{\mu}^{\alpha(k)}}_{\geq 0} \geq 0 \end{aligned} \quad (17)$$

The last two terms on the right hand side of Eq. (17) are not negative, the former due to the semi-definite positiveness of $\tilde{\mathbf{F}}$ and the latter due to the convexity of the elastic domain. As also $\Delta\xi^{(k)} > 0$ the sequence so generated does not decrease in λ . In the case $\lambda^{(k)} = \lambda^{(k-1)}$ with $\Delta\tilde{\mathbf{u}} \neq \mathbf{0}$ Eq. (17) implies $\Delta\tilde{\mathbf{t}} = \mathbf{0}$ and then also the requirements of the dual theorems (15a) are satisfied from Eq. (16c), that is the convergence to the desired shakedown multiplier. We call this kind of analysis *pseudo elastoplastic*, due to its meaning in the case of fixed loads.

3.2.2 The Mathematical Programming and Mechanical Interpretation of the Pseudo-elastoplastic Analysis

Each step in Eq. (16a) is obtained, apart from the inessential scaling of $\lambda^{(k)}$, by subtracting from the objective function of the static theorem a quadratic positive function in $\Delta\tilde{\mathbf{t}}$. In this respect it can be seen as a particular application of the proximal point algorithm (see Bertsekas [7] pp. 248 and [18, 19]) for solving Eq. (12c), i.e. the optimum solution of the static theorem is obtained by generating a convergent sequence of primal admissible solutions. The algorithm becomes competitive with direct methods if the sequence of steps is efficiently and robustly solved. This is possible by reusing the consolidated strain driven path-following algorithms adopted in elasto-plasticity [3].

Independently of this mathematical programming point of view, first order conditions in Eq. (16c) also have an important mechanical sense: in the fixed load case they define the standard finite step holonomic problem obtained by using a backward Euler scheme for integrating the constitutive elasto-plastic relationships. In this case $\Delta\mathbf{u}^{(k)}$ can be identified with the displacement step increment and the succession of point $\mathbf{z}^{(k)}$ with the equilibrium path. This holonomic transformation, with the irreversible phenomena that can now occur only at the beginning of each new

step, is widely adopted in elasto-plastic analysis. Its use is theoretically justified by the Ponter and Martin [20] extremal path theory that gives a clear mechanical sense to the so evaluated equilibrium path, allowing also the use of the kinematical part of the solution. A similar meaning can also be given for the shakedown case when the following expression of $\tilde{\mathbf{F}}$ is used

$$\tilde{\mathbf{F}} := \text{blockdiag}[\mathbf{F}, \mathbf{0}, \dots, \mathbf{0}] \quad (18)$$

In this case Eq. (16c) corresponds to a backward Euler integration scheme of the elasto-plastic equations for a load moving for all vertexes of the monotonously amplified load domain at each step of the analysis so allowing elastic adaptation. In this sense pseudo elasto-plastic analysis, apart from its mathematical programming interpretation, assumes a more general meaning overreaching the shakedown theorems and making the extension to more complex materials simple.

Finally note that, when interest is only in the shakedown multiplier, matrices \mathbf{F}^α , according to the global semi-definite property of $\tilde{\mathbf{F}}$, can be selected in order to simplify the computations.

4 Numerical Methods for the Evaluation of the Shakedown Multiplier

The proximal point algorithm in Eq. (16a)–(16c) can be efficiently solved by means of decomposition techniques, similar to that employed by Kaneko and Ha [19]. In this way a standard strain driven arc length formulation based on a return mapping by closest point projection scheme, such as that currently used to evaluate the equilibrium path of elasto-plastic structures, is obtained. This mathematical programming approach allows a direct comparison between the strain driven algorithm and direct global solvers in terms of performance and robustness. For a review of decomposition methods in optimization refer to Chap. 6 of Bertsekas [7] and Boyd's course lectures EE364b [5].

4.1 The Multisurface Decomposition

By selecting $\tilde{\mathbf{F}}$ as in Eq. (18) and omitting the index k and dependence on $\mathbf{z}^{(k-1)}$ to simplify the notation, the proximal point algorithm in Eq. (16a) becomes:

$$\begin{aligned} \max \quad & \Delta\xi\lambda - \frac{1}{2} \sum_{g=1}^{N_\sigma} \Delta\boldsymbol{\sigma}_g^T \mathbf{F}_g \Delta\boldsymbol{\sigma}_g \\ \text{subj.} \quad & \mathbf{Q}^T \mathbf{t} = \lambda \mathbf{p} \\ & f^\alpha[\boldsymbol{\sigma}_g, \lambda] \leq 0 \quad \forall \alpha, g \end{aligned} \quad (19a)$$

where the linear equality constraints have been directly substituted.

The complicating equilibrium equation constraints can be eliminated using a dual decomposition strategy, that is by adding them to the objective function forming the following partial Lagrangian:

$$\begin{aligned} \max \quad & \mathcal{L} \equiv \mathcal{L}_\lambda[\lambda, \mathbf{u}] + \sum_{g=1}^{N_\sigma} \mathcal{L}_g[\boldsymbol{\sigma}_g, \mathbf{u}] \\ \text{subj.} \quad & f^\alpha[\boldsymbol{\sigma}_g, \lambda] \leq 0 \quad \forall \alpha, g \end{aligned} \quad (19b)$$

where

$$\mathcal{L}_\lambda \equiv \lambda(\Delta \xi - \mathbf{p}^T \Delta \mathbf{u}), \quad \mathcal{L}_g \equiv \boldsymbol{\sigma}_g^T \boldsymbol{\varepsilon}_g[\Delta \mathbf{u}] - \frac{1}{2} \Delta \boldsymbol{\sigma}_g^T \mathbf{F}_g \Delta \boldsymbol{\sigma}_g$$

with $\Delta \mathbf{u}$ the vector of the Lagrange multiplier and $\boldsymbol{\varepsilon}_g[\Delta \mathbf{u}]$ the g th component of $\mathbf{Q} \Delta \mathbf{u}$.

The dual of problem (19b) is obtained maximizing \mathcal{L} with respect to the primal variables:

$$\mathcal{D}[\mathbf{u}] := \max_{\lambda} \left(\mathcal{L}_\lambda[\lambda, \mathbf{u}] + \sum_{g=1}^{N_\sigma} \max_{\substack{\boldsymbol{\sigma}_g, \\ f^\alpha[\boldsymbol{\sigma}_g, \lambda] \leq 0}} \mathcal{L}_g[\boldsymbol{\sigma}_g, \mathbf{u}] \right) \quad (19c)$$

that is now separated for limit analysis while it still has the complicating variables λ that prevent its decomposition for shakedown. The dual function is evaluated by fixing λ and performing the maximization with respect to $\boldsymbol{\sigma}_g$ so obtaining the following, strictly convex, minimization problems for each stress point g

$$\mathcal{D}_g[\lambda, \mathbf{u}] := \begin{cases} \min_{(\boldsymbol{\sigma}_g)} & \frac{1}{2} (\boldsymbol{\sigma}_g - \boldsymbol{\sigma}_g^*)^T \mathbf{F}_g (\boldsymbol{\sigma}_g - \boldsymbol{\sigma}_g^*) \\ \text{subj.} & \mathbf{f}_s[\boldsymbol{\sigma}_g, \lambda] := [f^1[\boldsymbol{\sigma}_g, \lambda], \dots, f^{N_v}[\boldsymbol{\sigma}_g, \lambda]]^T \leq \mathbf{0} \end{cases} \quad (19d)$$

where the trial stress defined as $\boldsymbol{\sigma}_g^* = \boldsymbol{\sigma}_g^{(k-1)} + \mathbf{F}_g^{-1} \boldsymbol{\varepsilon}_g$. Equation (19d) is a small convex problem in $n_\sigma := \dim\{\boldsymbol{\sigma}_g\}$ variables subject to N_v nonlinear constraints and its solution can be easily performed by means of a *Sequential Quadratic Programming* method (SQP). Each QP problem is, in this work, efficiently solved with the Goldfarb-Idnani dual active set method [25] already used in [4].

Finally the solution of (19a) is obtained by solving the following unconstrained problem:

$$\mathcal{D} := \min_{\Delta \mathbf{u}} \mathcal{D}[\mathbf{u}] = \min_{\Delta \mathbf{u}} \max_{\lambda} \left(\mathcal{L}_\lambda[\lambda, \mathbf{u}] - \sum_{g=1}^{N_\sigma} \mathcal{D}_g[\lambda, \mathbf{u}] \right) \quad (19e)$$

In the limit analysis case the objective function is independent of λ and the minimization is performed only with respect to \mathbf{u} .

The initial problem in (16a) is solved through its dual (19e) that is a free optimization problem nested within a series of simple convex projections (19d) of the

trial stresses in the admissible domain. Denoting with a comma the derivation with respect to the quantity that follows as subscript, and referring to Sect. 6.1 of [7] for the evaluation of the gradient of the dual function, the first order conditions of Eq. (19e) are

$$\mathbf{r}_{eq} \equiv \mathbf{Q}^T \mathbf{t}[\lambda, \mathbf{u}] - \lambda \mathbf{p} = \mathbf{0}, \quad r_\lambda \equiv \mathbf{p}^T \Delta \mathbf{u} + \sum_g \mu_{sg}^T \mathbf{f}_s[\sigma_g, \lambda]_{,\lambda} - \Delta \xi = 0 \quad (19f)$$

where $\mathbf{t}[\lambda, \mathbf{u}]$ collects all $\sigma_g[\lambda, \mathbf{u}]$ solutions of problems (19d) while $\mu_{sg} = [\mu_{sg}^1, \dots, \mu_{sg}^{N_v}]$ are the Lagrange multipliers associated with the inequality constraints. The stress is univocally defined in terms of $\Delta \mathbf{u}$ and λ , using Eq. (19d) that so represents an implicit nonlinear elastic constitutive law, the past history being contained in $\mathbf{z}^{(k-1)}$. The strict convexity of the problems (19d) makes the dual function differentiable and then solvable using a Newton method expressed only in terms of the configuration variables λ and \mathbf{u} . Equations (19f) are the standard equilibrium equations and the arc-length constraints in Table 1, making it easy to show that

$$\sum_g \mu_{sg}^T \mathbf{f}_{s,\lambda} = \sum_{\beta=2}^{N_v} (\Delta \rho)^\beta \mathbf{t}^{E\beta}$$

Finally note that an alternative equivalent formulation for Eq. (19e) is

$$\begin{cases} \min_{\Delta \mathbf{u}} & \mathcal{D}[\mathbf{u}] \\ \text{subj.} & \mathbf{p}^T \Delta \mathbf{u} + \sum_g \mu_g^T \mathbf{f}_{s,\lambda} - \Delta \xi = 0 \end{cases} \quad (19g)$$

4.2 A Further Decomposition Technique

Another possible decomposition technique is obtained relaxing all the complicating constraints defined, in Eq. (16c), by the extended equilibrium equations. Letting $\Delta \tilde{\mathbf{u}}$ be the Lagrange multiplier associated with the relaxed constraint and now making $\mathbf{F}^\alpha = \mathbf{F}$ for all vertexes, with $c \in \mathbb{R}^+$ a suitable scale factor, we obtain

$$\begin{aligned} & \text{maximize} \quad \mathcal{L}_\lambda[\lambda, \Delta \tilde{\mathbf{u}}] + \sum_{\alpha=1}^{N_v} \sum_{g=1}^{N\sigma} \mathcal{L}_g^\alpha[\tilde{\mathbf{t}}, \Delta \tilde{\mathbf{u}}] \\ & \text{subject to} \quad f^\alpha[\sigma_g^\alpha] \leq 0 \quad \forall \alpha, g \end{aligned} \quad (20a)$$

where now

$$\mathcal{L}_\lambda := \lambda(\Delta \xi - \Delta \tilde{\mathbf{u}}^T \tilde{\mathbf{p}}), \quad \mathcal{L}_g^\alpha[\tilde{\mathbf{t}}, \Delta \tilde{\mathbf{u}}] := \frac{1}{2}(\sigma_g^\alpha)^T \mathbf{F}_g \sigma_g^\alpha - (\sigma_g^\alpha)^T \mathbf{e}_g^\alpha$$

σ_g^α and ε_g^α are the g th component of \mathbf{t}^α and $\Delta \boldsymbol{\rho}^\alpha$ respectively and $\Delta \boldsymbol{\rho}^1 = \mathbf{Q} \Delta \mathbf{u}$.

In this case too the problem is separable and it is possible to maximize function $\mathcal{L}_{g\alpha}$, at each stress point sub-level and for each α , as follows

$$\mathcal{D}_g^\alpha[\Delta \tilde{\mathbf{u}}] := \begin{cases} \min_{(\sigma_g^\alpha)} & \frac{1}{2} (\sigma_g^\alpha - \sigma_g^{\alpha*})^T \mathbf{F}_g (\sigma_g^\alpha - \sigma_g^{\alpha*}) \\ \text{subj.} & f[\sigma_g^\alpha] \leq 0 \end{cases} \quad (20b)$$

where the trial stress is now defined as $\sigma_g^{\alpha*} = (\sigma_g^\alpha)^{(k-1)} + \mathbf{F}_g^{-1} \Delta \varepsilon_g^\alpha$.

The initial problem in (16a) is then transformed into the following free minimization problem

$$\mathcal{D}[\tilde{\mathbf{u}}] : \begin{cases} \min_{\Delta \tilde{\mathbf{u}}} & \left\{ \sum_{g,\alpha} \mathcal{D}_g^\alpha[\Delta \tilde{\mathbf{u}}] \right\} \\ \text{subj.} & \Delta \tilde{\mathbf{u}}^T \tilde{\mathbf{p}} = \Delta \xi \end{cases} \quad (20c)$$

nested within a series of simple convex projections (20b) of the trial stresses in the admissible domain. The first order conditions for (20c) represent the extended equilibrium equation plus the arc-length constraint and are

$$\tilde{\mathbf{r}}_{eq}[\lambda, \tilde{\mathbf{u}}] := \tilde{\mathbf{Q}}^T \tilde{\mathbf{t}}[\Delta \tilde{\mathbf{u}}] - \lambda \tilde{\mathbf{p}} = \mathbf{0}, \quad r_\lambda[\lambda, \tilde{\mathbf{u}}] := \Delta \xi - \Delta \tilde{\mathbf{u}}^T \tilde{\mathbf{p}} = 0 \quad (20d)$$

with the stress $\mathbf{t}[\tilde{\mathbf{u}}]$ univocally defined in terms of $\Delta \tilde{\mathbf{u}}$ by using (20b). They can be solved iteratively using a Newton scheme. The other equations in Table 1 are solved exactly using Eq. (20b) for each assigned value of $\Delta \tilde{\mathbf{u}}$. Note also that this formulation is more decoupled with respect to the previous one and will be called SS-SD.

4.3 Final Considerations

Strain driven methods, apart from their classic interpretation, can be seen as decomposition strategies well suited for use within the proximal point algorithm. They solve, through a Newton method, the free dual problem obtained by means of a series of very small optimization subproblems (the closest point projection schemes) for each new estimate of the configuration variables. Stresses and other locally defined quantities then become functions of the configuration variables and the problem description is always compatible and usually highly nonlinear, even when the finite element is mixed. For a deeper discussion of how the problem description affects the convergence in Newton methods the reader is referred to [23]. The method fully exploits the information gained from the previously evaluated step handling the problem nonlinearity by means of adaptive arc-length selections. In the fixed load case both the above decomposition strategies are exactly the same.

5 Numerical Implementation of Strain Driven Methods

The implementational aspects of the numerical strategies previously proposed are now discussed. Readers are referred to [3, 4, 23] for details of the arc-length path-following strategies.

5.1 The Global Solution Scheme

Equations (19f) and (20d) are solved using a Newton method that, by means of block elimination of the local defined variables, can be expressed in a common *pseudo-compatible* format in terms of (\mathbf{u}, λ) alone:

$$\begin{bmatrix} \mathbf{K}_j & -\mathbf{y}_j \\ -\mathbf{y}_j^T & h_j \end{bmatrix} \begin{bmatrix} \dot{\mathbf{u}} \\ \dot{\lambda} \end{bmatrix} = - \begin{bmatrix} \hat{\mathbf{r}}_{eq} \\ \hat{r}_\lambda \end{bmatrix} \quad (21a)$$

where subscript j denotes quantities evaluated in the current iteration and

$$\mathbf{K}_j = \mathbf{Q}^T \mathbf{E}_t \mathbf{Q}, \quad \mathbf{y}_j = \mathbf{p} + \mathbf{Q}^T \mathbf{t}_\lambda, \quad \hat{\mathbf{r}}_{eq} = \mathbf{r}_{eqj} + \mathbf{r}_{eq}^c, \quad \hat{r}_\lambda = r_{\lambda j} + r_\lambda^c \quad (21b)$$

with \mathbf{E}_t , \mathbf{t}_λ , h_j , \mathbf{r}_{eq}^c and r_λ^c having a different expression depending on the algorithm in use. \mathbf{E}_t always maintains the following local level block diagonal structure

$$\mathbf{E}_t = \text{blockdiag}[\mathbf{E}_{t1}, \dots, \mathbf{E}_{tN_\sigma}] \quad (21c)$$

and is obtained by means of a standard FEM assemblage of local contributions.

The solution of Eq. (21a) is

$$\dot{\mathbf{u}} = \dot{\lambda} \hat{\mathbf{u}} + \bar{\mathbf{u}}, \quad \dot{\lambda} = \frac{\hat{r}_\lambda - \mathbf{y}_j^T \bar{\mathbf{u}}}{(\mathbf{y}_j^T \hat{\mathbf{u}} - h_j)} \quad \text{where} \quad \begin{cases} \hat{\mathbf{u}} = \mathbf{K}_j^{-1} \mathbf{y}_j \\ \bar{\mathbf{u}} = -\mathbf{K}_j^{-1} \hat{\mathbf{r}}_{eq} \end{cases} \quad (21d)$$

Equations in (21a)–(21d) have the same format as a standard arc length nonlinear analysis [3, 23], its solution having the same computational cost for both methods and in both cases of shakedown or limit analysis. The differences lie only in the local level operations which, involving only few variables, are cheaper to perform.

5.2 Numerical Implementation of the MS-RM Formulation

Letting $\mathbf{z}_0 := \mathbf{z}^{(k-1)}$, the scheme produces a sequence of plastically admissible estimates \mathbf{z}_j , convergent to the new state $\mathbf{z}^{(k)}$, by recursively updating the configuration variables as:

$$\mathbf{u}_{j+1} := \mathbf{u}_j + \dot{\mathbf{u}}_j, \quad \lambda_{j+1} := \lambda_j + \dot{\lambda}_j \quad (22)$$

with $\dot{\mathbf{u}}_j$ and $\dot{\lambda}_j$ evaluated according to (21a)–(21d) and the other local variables using the return mapping process Eq. (19d). From the linearization of the first order conditions Eq. (19f) with respect to λ and \mathbf{u} we obtain:

$$\begin{aligned} \mathbf{E}_t &= \frac{\partial \mathbf{t}}{\partial \boldsymbol{\rho}} = \text{blockdiag}[\mathbf{E}_{t1}, \dots, \mathbf{E}_{tN_\sigma}], & \mathbf{E}_{tg} &:= \frac{\partial \boldsymbol{\sigma}_g}{\partial \boldsymbol{\varepsilon}_g} \\ \mathbf{t}_\lambda &:= -\frac{\partial \mathbf{t}}{\partial \lambda} = - \begin{bmatrix} \boldsymbol{\sigma}_{1,\lambda} \\ \vdots \\ \boldsymbol{\sigma}_{N_\sigma,\lambda} \end{bmatrix} \\ \boldsymbol{\sigma}_{g,\lambda} &:= \frac{\partial \boldsymbol{\sigma}_g}{\partial \lambda}, & h_j &= - \sum_{g=1}^{N_\sigma} (\boldsymbol{\mu}_g^T \mathbf{f}_{sg,\lambda\lambda} + \mathbf{f}_{sg,\lambda}^T \boldsymbol{\mu}_{g,\lambda}) \end{aligned} \quad (23)$$

where $\boldsymbol{\rho} = \mathbf{Q}\Delta\mathbf{u}_j$ and $\boldsymbol{\varepsilon}_g$ is its g th component and both $\mathbf{r}_{eq}^c \equiv \mathbf{0}$, $r_\lambda^c = 0$.

The sequence so generated is locally convergent due to the presence of the arc-length condition that allows (21a) to be solved even when \mathbf{K}_j becomes singular as happens near the shakedown or the limit load multiplier [3, 23]. For global convergence we can set \mathbf{K}_j as equal to the initial elastic matrix \mathbf{K}_E . In this way while the quadratic convergence rate of the Newton method is lost we avoid the matrix decomposition for each \mathbf{z}_j . Alternatively a line search algorithm can be useful.

5.2.1 Evaluation of the Incremental Quantities for MS-RM

The algorithmic tangent moduli can be obtained from the second derivatives of the dual function once the internal variables are eliminated or, following an approach more common in the computational mechanics community, by the consistent linearization of the return mapping process. Making $n_a > 0$ the number of active constraints, and keeping the notation used to indicate quantities in this active subset unchanged, the first order condition defined by (19d) can be rewritten as

$$\begin{cases} \dot{\boldsymbol{\sigma}}_g = \mathbf{H}_g^{-1} (\dot{\boldsymbol{\varepsilon}}_g - \mathbf{A}_{sg} \dot{\boldsymbol{\mu}}_{sg} - \dot{\lambda} \mathbf{A}_{sg,\lambda} \boldsymbol{\mu}_{sg}) \\ \mathbf{A}_{sg}^T \dot{\boldsymbol{\sigma}}_g + \dot{\lambda} \mathbf{f}_{sg,\lambda} = \mathbf{0} \end{cases}$$

where $\boldsymbol{\mu}_{sg}^T = [\mu_{sg}^1, \dots, \mu_{sg}^{n_a}]$ and

$$\mathbf{A}_{sg} = \left[\frac{\partial f^1}{\partial \boldsymbol{\sigma}_g} \dots \frac{\partial f^{n_a}}{\partial \boldsymbol{\sigma}_g} \right], \quad \mathbf{H}_g[\boldsymbol{\sigma}_g] = \mathbf{F}_g + \sum_{\alpha=1}^{n_a} \mu_{sg}^\alpha \frac{\partial^2 f^\alpha}{\partial \boldsymbol{\sigma}_g^2} \quad (24)$$

Making $\mathbf{W}_g = (\mathbf{A}_{sg}^T \mathbf{H}_g^{-1} \mathbf{A}_{sg})^{-1}$ we obtain the required quantities

$$\begin{aligned} \mathbf{E}_{tg} &= \mathbf{H}_g^{-1} - \mathbf{H}_g^{-1} \mathbf{A}_{sg} \mathbf{W}_g \mathbf{A}_{sg}^T \mathbf{H}_g^{-1} \\ \boldsymbol{\sigma}_{g,\lambda} &= -\mathbf{H}_g^{-1} \mathbf{A}_{sg} \mathbf{W}_g \mathbf{f}_{sg,\lambda} - \mathbf{E}_{tg} \mathbf{A}_{sg,\lambda} \boldsymbol{\mu}_{sg} \end{aligned} \quad (25)$$

Note that \mathbf{E}_{tg} and $\mathbf{H}_j^{-1} \mathbf{A}_{sg} \mathbf{W}_g$ are directly furnished by the QP solution scheme used to solve Eq. (19d) so only $\mathbf{f}_{gs,\lambda}$, $\mathbf{f}_{gs,\lambda\lambda}$ and $\mathbf{A}_{sg,\lambda}$ need to be evaluated. Also note that for $n_a = 0$, we have the elastic step.

5.3 Numerical Implementation of the SS-RM Algorithm

Starting from $\mathbf{z}_0 := \mathbf{z}^{(k-1)}$, the scheme produces once more a sequence of estimates \mathbf{z}_j updating the configuration variables as:

$$\tilde{\mathbf{u}}_{j+1} := \tilde{\mathbf{u}}_j + \dot{\tilde{\mathbf{u}}}_j, \quad \lambda_{j+1} := \lambda_j + \dot{\lambda}_j \quad (26a)$$

where $\dot{\tilde{\mathbf{u}}}_j$ and $\dot{\lambda}_j$ now satisfy, the first order approximation of (20d):

$$\begin{bmatrix} \tilde{\mathbf{K}}_j & -\tilde{\mathbf{p}} \\ -\tilde{\mathbf{p}}^T & 0 \end{bmatrix} \begin{bmatrix} \dot{\tilde{\mathbf{u}}} \\ \dot{\lambda} \end{bmatrix} = - \begin{bmatrix} \tilde{\mathbf{r}}_{eq}^c \\ r_{\lambda j} \end{bmatrix} \quad (26b)$$

In the previous equation $\tilde{\mathbf{r}}_{eq}^c = \tilde{\mathbf{r}}_{eqj}$ and

$$\tilde{\mathbf{K}}_j = \tilde{\mathbf{Q}}^T \tilde{\mathbf{E}}_t \tilde{\mathbf{Q}}, \quad \tilde{\mathbf{E}}_t := \text{blockdiag}\{\mathbf{E}_t^1, \dots, \mathbf{E}_t^{N_v}\}$$

where, letting $\boldsymbol{\rho}_1 = \mathbf{Q} \Delta \mathbf{u}_j$, we have:

$$\mathbf{E}_t^\alpha := \frac{\partial \mathbf{t}^\alpha}{\partial \boldsymbol{\rho}^\alpha} = \text{blockdiag}\{\mathbf{E}_{t1}^1, \dots, \mathbf{E}_{tN_\sigma}^{N_v}\}, \quad \mathbf{E}_{tg}^\alpha = \frac{\partial \boldsymbol{\sigma}_g^\alpha}{\partial \boldsymbol{\varepsilon}_g^\alpha}$$

$\tilde{\mathbf{E}}_t$ is a block diagonal matrix with each block \mathbf{E}_t^α in turn blockdiagonal and defined by the consistent linearization of the return mapping algorithm (20b) (or of the dual function) as:

$$\mathbf{E}_{tg}^\alpha := \begin{cases} (\mathbf{H}_g^\alpha)^{-1} (\mathbf{I} - \frac{\mathbf{a}^\alpha \mathbf{a}^{\alpha T} (\mathbf{H}_g^\alpha)^{-1}}{h + (\mathbf{a}^\alpha)^T (\mathbf{H}_g^\alpha)^{-1} \mathbf{a}^\alpha}) & \text{if } \mu_g^\alpha > 0 \\ \mathbf{F}_g^{-1} & \text{otherwise} \end{cases} \quad (26c)$$

where now

$$\mathbf{a}^\alpha = \frac{\partial f[\boldsymbol{\sigma}_g^\alpha]}{\partial \boldsymbol{\sigma}_g^\alpha}, \quad \mathbf{H}_g^\alpha = \mathbf{F}_g + \mu_g^\alpha \frac{\partial^2 f[\boldsymbol{\sigma}_g^\alpha]}{\partial (\boldsymbol{\sigma}_g^\alpha)^2}$$

and $h \simeq 1.0^{-4} - 1.0^{-6}$ is used to avoid singularity.

5.3.1 The Partitioned Solution Scheme

Recalling the definition of $\tilde{\mathbf{Q}}$ and of $\tilde{\mathbf{p}}$ in Eqs. (13), (14), the system in (26b) becomes

$$\begin{bmatrix} \mathbf{K}_{\rho\rho} & \mathbf{K}_{u\rho}^T & -\mathbf{t}_\rho \\ \mathbf{K}_{u\rho} & \mathbf{K}_{uu} & -\mathbf{p} \\ -\mathbf{t}_\rho^T & -\mathbf{p}^T & 0 \end{bmatrix} \begin{bmatrix} \dot{\boldsymbol{\rho}} \\ \dot{\mathbf{u}} \\ \dot{\lambda} \end{bmatrix} = - \begin{bmatrix} \mathbf{r}_{eq\rho} \\ \mathbf{r}_{eq} \\ r_\lambda \end{bmatrix} \quad (27a)$$

where

$$\mathbf{r}_{eq} = \mathbf{Q}^T \mathbf{t}_j - \lambda_j \mathbf{p}, \quad r_\lambda = \Delta \xi - \mathbf{p}^T \Delta \mathbf{u}_j - \Delta \boldsymbol{\rho}_j^T \mathbf{t}^E \quad (27b)$$

$$\mathbf{r}_{eq\rho} = \begin{bmatrix} \mathbf{t}^2 - \mathbf{t} - \lambda \mathbf{t}^{E2} \\ \vdots \\ \mathbf{t}^{N_v} - \mathbf{t} - \lambda \mathbf{t}^{EN_v} \end{bmatrix} = \begin{bmatrix} \mathbf{r}_{eq}^2 \\ \vdots \\ \mathbf{r}_{eq}^{N_v} \end{bmatrix} \quad (27c)$$

and

$$\mathbf{K}_{uu} = \mathbf{Q}^T \mathbf{E}_t^1 \mathbf{Q}, \quad \mathbf{K}_{u\rho} = -\mathbf{Q}^T \mathbf{E}_t^1 \boldsymbol{\Sigma}, \quad \mathbf{K}_{\rho\rho} = \boldsymbol{\Sigma}^T \mathbf{E}_t^1 \boldsymbol{\Sigma} + \mathbf{E}_\rho \quad (27d)$$

with

$$\mathbf{E}_\rho := \text{blockdiag} \begin{bmatrix} \mathbf{E}_t^2 & \dots & \mathbf{E}_t^{N_v} \end{bmatrix}. \quad (27e)$$

By a block elimination of $\dot{\boldsymbol{\rho}}$, performed at the local level due to the block diagonal structure of $\mathbf{K}_{\rho\rho}$ we obtain the global scheme in the form of Eqs. (21a)–(21d). To avoid the inversion of $\mathbf{K}_{\rho\rho}$, that could be computationally expensive for high values of N_v , it is convenient to use the Woodbury matrix identity so obtaining:

$$\mathbf{K}_{\rho\rho}^{-1} = \mathbf{E}_\rho^{-1} - \mathbf{E}_\rho^{-1} \boldsymbol{\Sigma}^T \mathbf{F}_t^{-1} \boldsymbol{\Sigma} \mathbf{E}_\rho^{-1} \quad \text{with } \mathbf{F}_t = \sum_{\alpha=1}^{N_v} \mathbf{F}_t^\alpha$$

where

$$\mathbf{F}_t^\alpha \equiv (\mathbf{E}_t^\alpha)^{-1} = \text{blockdiag} \{ (\mathbf{E}_{t1}^\alpha)^{-1}, \dots, (\mathbf{E}_{tN_\sigma}^\alpha)^{-1} \}$$

Letting

$$\mathbf{q} = \sum_{\beta=2}^{N_v} \mathbf{F}_t^\beta \mathbf{t}^{E\beta}, \quad \mathbf{r}_q = \sum_{\beta=2}^{N_v} \mathbf{F}_t^\beta \mathbf{r}_{eq}^\beta \quad (28)$$

with some substitutions we obtain the following expression for the quantities in Eqs. (21a)–(21d)

$$\begin{aligned} \mathbf{E}_t &= \mathbf{F}_t^{-1}, & \mathbf{t}_\lambda &= \mathbf{E}_t \mathbf{q}, & h_j &= \mathbf{q}^T \mathbf{E}_t \mathbf{q} - \sum_{\beta=2}^{N_v} (\mathbf{t}^{E\beta})^T \mathbf{F}_t^\beta \mathbf{t}^{E\beta} \\ \mathbf{r}_{eq}^c &= \mathbf{Q}^T \mathbf{E}_t \mathbf{r}_q, & r_\lambda^c &= \sum_{\beta} (\mathbf{r}_{eq\rho}^\beta)^T \mathbf{F}_t^\beta \mathbf{t}^{E\beta} - \mathbf{q}^T \mathbf{E}_t \mathbf{r}_q \end{aligned} \quad (29)$$

and from back-substitution

$$\dot{\rho}_\beta = \mathbf{F}_t^\beta (\dot{\lambda} \mathbf{t}^{E\beta} - \mathbf{r}_{eq}^\beta - \mathbf{E}_t (\dot{\lambda} \mathbf{q} - \rho^1 - \mathbf{r}_q))$$

Finally note that for a purely elastic behavior we obtain

$$\mathbf{E}_t = \frac{1}{c} \mathbf{F}^{-1}, \quad c = N_v$$

that is, with an appropriate selection of \mathbf{F} we can use, at the global level, \mathbf{K}_E as iteration matrix obtaining, also in this case, a global convergent scheme.

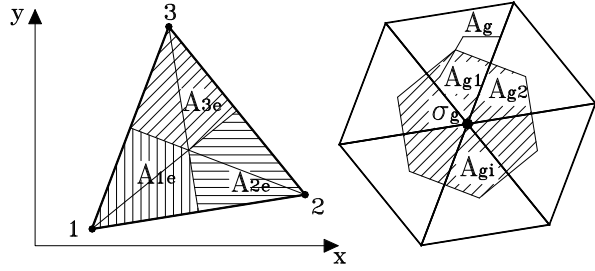
6 The Finite Element Discretization

A finite element suitable for shakedown analysis needs to be accurate with respect to both the evaluation of the elastic envelope stress $\mathbf{t}^{E\alpha}$ necessary for the correct evaluation of $\bar{\lambda}$ and with respect to the description of the ratcheting mechanism that usually require fine meshes. In this work these rules have been satisfied by using two finite elements on different discretization grids. In particular, stresses $\mathbf{t}^{E\alpha}$ are evaluated using the standard eight node compatible quadrilateral isoparametric element Q_8 [26] while the complete shakedown analysis exploits the mixed SIMPLEX (S) finite element [4], free of volumetric locking and sufficiently simple to be used with fine mesh. Note that, apart from the mixed interpolation, the element is similar to that recently proposed in [21].

6.1 The Simplex Finite Element

We briefly recall the SIMPLEX element while referring readers to [4] for details. Body domain B is subdivided into triangular elements of area A_e and thickness h_e with three nodes, located at the vertices of a triangle. A simple bilinear interpolation for the displacements was adopted while the stresses are kept constant on the nodal influence area $A_g = \sum_e A_{ge}/3$, sum of the contributions $A_{ge}/3$ of each element linked to the node g (see Fig. 1).

Fig. 1 The Simplex finite element



The compatible strain $\boldsymbol{\varepsilon}_{ge}$ for each of the n_{ge} elements linked to the stress node g is constant and coincident with that of the compatible linear triangle T_3 . It can be expressed as

$$\boldsymbol{\varepsilon}_{ge} = \mathbf{D}_e \mathbf{d}_e \quad (30)$$

$\mathbf{d}_e = [\mathbf{u}_1, \mathbf{u}_2, \mathbf{u}_3]^T$ being the displacement element vector collecting the element node displacement vector \mathbf{u}_k . Denoting with $\mathbf{u}_g^T = [\mathbf{u}_{g1}, \mathbf{u}_{g2}, \dots, \mathbf{u}_{gn_e}]$ the stress node displacement vector, collecting the displacement vectors \mathbf{u}_{gi} of all the elements linked to the stress node g and letting \mathbf{A}_e be the matrix extracting the element displacements from \mathbf{d}_g

$$\mathbf{d}_e = \mathbf{A}_{ge} \mathbf{d}_g$$

we obtain the following algebraic form for the quantities required in the analysis:

$$\frac{1}{2} \int_V \boldsymbol{\sigma}^T \mathbf{E}^{-1} \boldsymbol{\sigma} dV = \frac{1}{2} \sum_{g=1}^{N_g} \boldsymbol{\sigma}_g^T \mathbf{F}_g \boldsymbol{\sigma}_g, \quad \int_V \boldsymbol{\sigma}^T \boldsymbol{\varepsilon} dV = \sum_{g=1}^{N_g} \boldsymbol{\sigma}_g^T \mathbf{D}_g \mathbf{u}_g \quad (31)$$

and the strain work conjugate with $\boldsymbol{\sigma}_g$ is now defined by the compatibility matrix

$$\mathbf{Q}_g = \sum_{e=1}^{n_{ge}} \mathbf{D}_e \mathbf{A}_{ge} V_{ge} / 3$$

where $V_{ge} = A_{ge} h_{ge}$ is the volume of the e th element linked with the stress node g and $V_g = \sum_{e=1}^{n_{ge}} V_{ge} / 3$ the total volume related to the stress node and $\mathbf{F}_g = \mathbf{E}^{-1} V_g$.

Letting $\mathbf{t} = [\boldsymbol{\sigma}_1, \dots, \boldsymbol{\sigma}_{N_\sigma}]^T$ and $\mathbf{u} = [\mathbf{u}_1, \dots, \mathbf{u}_{N_u}]^T$ be the global vectors collecting the N_σ nodal stresses and the N_u displacements and denoting with

$$\mathbf{d}_g = \mathbf{T}_{ug} \mathbf{u}, \quad \boldsymbol{\sigma}_g = \mathbf{T}_{\sigma g} \mathbf{t}$$

the operators linking local and global quantities we obtain

$$\mathbf{Q}^T \mathbf{t} \equiv \sum_g \mathbf{Q}_g^T \boldsymbol{\sigma}_g, \quad \mathbf{F} = \sum_g \mathbf{T}_{\sigma g}^T \mathbf{F}_g \mathbf{T}_{\sigma g} \quad \text{with } \mathbf{Q}_g = \mathbf{T}_{ug}^T \mathbf{D}_g.$$

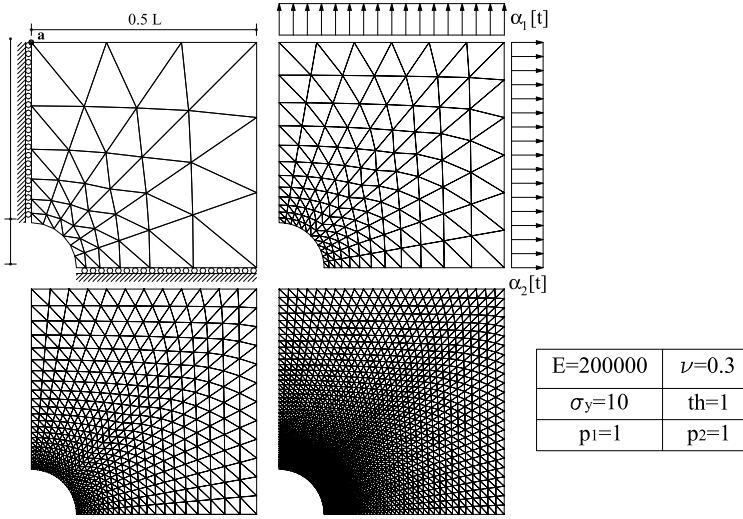


Fig. 2 Geometry and finite element mesh for the square plate

7 Numerical Results

The algorithms presented are compared in terms of accuracy, robustness and effectiveness with the interior point method implemented in the commercial software *MOSEK*, using both a SOCP and a quadratic description (QP) of the constraints. We denote with *MS-RM* and *SS-RM* the strain driven return mapping analysis results, the name of the method is followed by K_e to indicate that the initial elastic stiffness matrix for each iteration was used (modified Newton method). Due to the linear convergence rate of the modified Newton method, the tolerance on the equilibrium equation is set equal to $1.0^{-3} \times (\lambda_e \sqrt{\sum_i \mathbf{p}_i^T \mathbf{K}_e^{-1} \mathbf{p}_i} / N_v)$, that is not too strict but adequate to produce results affected by an error in λ_a no greater than 0.05 %.

For all tests we will denote with λ_c^i the limit load multiplier for the load combination obtained, for fixed values of α_k^i and corresponding to a given load domain vertex v^i . In this case, due to the coincidence of the formulations, we obtain the same behavior for the *MS-RM* and *SS-RM* algorithms.

7.1 Square Plate with a Central Circular Hole

The first test is the classic plate subject to the biaxial uniform loads p_1 and p_2 (see Fig. 2) considered in numerical shakedown analysis [27–29]. Letting $0 \leq \alpha_1 \leq 1$ and $0 \leq \alpha_2 \leq 1$, some limit analysis and shakedown cases were investigated.

The (6×3) , (12×6) , (24×12) and (48×24) grids denoted as *meshes* 1, 2, 3 and 4 respectively were used. The first term indicates the number of elements along the hole, the second that on the opposite boundary.

Table 2 Square plate: discretization error on different meshes. The λ_c values are relative to vertex $v_3 = (1, 0)$ while ($\lambda_a = \bar{\lambda}$). Results are multiplied by 10

	<i>mesh 1</i>		<i>mesh 2</i>		<i>mesh 3</i>		<i>mesh 4</i>	
	λ_c^3	$\bar{\lambda}$	λ_c^3	λ_a	λ_c^3	λ_a	λ_c^3	λ_a
Q_8	8.060	4.333	8.020	4.315	8.008	4.305	8.003	4.302

Table 3 Comparison of λ_c and λ_a values for the square plate

(p_1, p_2)	λ_c			λ_a		
	(1, 1)	(1, 0.5)	(1, 0)	(1, 1)	(1, 0.5)	(1, 0)
Stein et al. [29]	–	–	0.802	0.453	0.539	0.624
Zhang et al. [30]	0.893	0.907	0.789	0.477	0.549	0.647
Gross-Weege [27]	0.882	0.891	0.782	0.446	0.524	0.614
Silveira [28]	0.894	0.911	0.803	0.429	0.500	0.594
Krabbenhøft et al. [11]				0.430	0.499	0.595
Garcea et al. [4]	0.902	0.912	0.806	0.438	0.508	0.604
Present (<i>mesh 4</i>)	0.895	0.911	0.800	0.430	0.499	0.595

Table 4 Square Plate: comparison of performance between the algorithms. Limit analysis is performed for vertex load $v_4 = (1.0, 1.0)$. In parentheses the number of steps

	MESH 3				MESH 4			
	λ_c^4		λ_a		λ_c^4		λ_a	
	CPU	loop	CPU	loop	CPU	loop	CPU	loop
<i>MS-RM</i>	5.25	118(31)	0.27	9(2)	31.55	146(39)	1.72	5(2)
<i>MS-RM-K_e</i>	11.26	786(64)	0.10	16(2)	23.19	755(68)	0.38	14(2)
<i>SS-RM</i>	5.25	118(31)	0.40	10(3)	31.55	146(39)	1.96	7(3)
<i>SS-RM-K_e</i>	11.26	786(64)	0.73	32(3)	23.19	755(68)	1.87	31(3)
MOSEK	0.44	15	1.73	14	2.20	13	8.14	10
MOSEK QP	0.62	19	2.02	10	4.64	22	33.70	12

In Table 4 the CPU time, the number of iterations and the number of values of safe state $\mathbf{z}^{(k)}$ (step), evaluated by the proximal point algorithm, are reported. In all cases the values of both the static and kinematic multiplier are coincident and some of them are reported in Table 2. A comparison with some of the results existing in literature is reported in Table 3.

In this example, due to the occurrence $\lambda = \bar{\lambda}$, we have practically the same performance between the *MS-RM* and *SS-RM* analysis also in the shakedown case, with the strain driven procedures more effective than IPM. Obviously this is only due to the practically elastic behavior of the structures for such values of the multiplier. With respect to CPU, at least in the evaluation of the limit analysis multiplier, our implementation pays the greater cost of the single iteration, in MOSEK performed using carefully tuned and very efficient routines for sparse linear algebra.

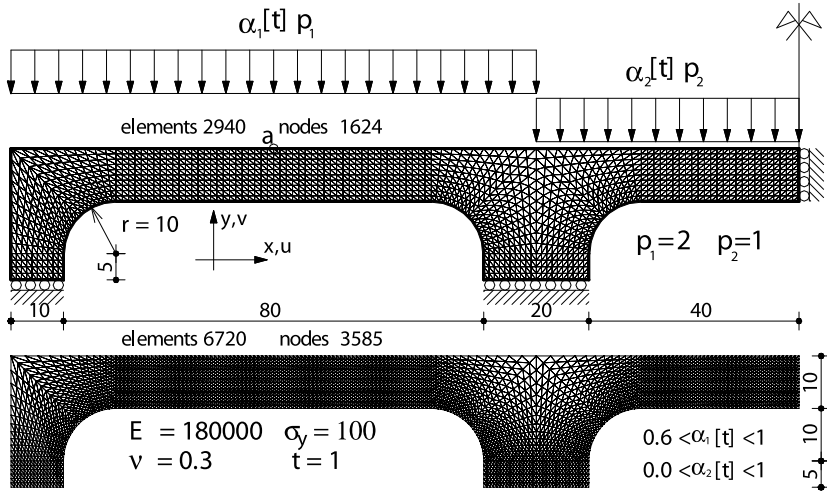


Fig. 3 Geometry and finite element grid for continuous beam

Table 5 Values of the collapse and shakedown multipliers for continuous beam. $v_2 = (0.6, 1)$, $v_3 = (1, 0)$

mesh 1					mesh 2				
λ_e	λ_a	$\bar{\lambda}$	λ_c^2	λ_c^3	λ_e	λ_a	$\bar{\lambda}$	λ_c^2	λ_c^3
1.281	3.143	5.995	5.330	3.198	1.276	3.166	5.971	5.368	3.221

7.2 A Symmetric Continuous Beam

The analysis regards the structure, whose geometry, load domain, material properties and the two discretization meshes used (*mesh 1* and *mesh 2*) are reported in Fig. 3. In this case we have ratcheting collapse, that is $\lambda_a < \lambda_c^i < \bar{\lambda}$. Shakedown and the lower limit load multipliers for the two different meshes are reported in Table 5.

In Table 6 performances of the various implementations are reported. Shakedown or limit load multipliers are more effectively evaluated using MOSEK and the *MS-RM* has an overall better behavior with respect to the *SS-RM* that exhibits its worst performances when the tangent matrix is used. Finally the cost of each iteration is highly affected by the number of constraints when using MOSEK.

8 Conclusions

In this work, it has been shown how standard incremental elastoplastic analysis based on closest point projection return mapping schemes, can be obtained from a mathematical programming problem, consisting in the application of the proximal

Table 6 Continuous beam: comparison of performance between the algorithms. Limit analysis is performed for vertex load $v_2 = (0.6, 1.0)$. In parentheses the number of steps

	MESH 1				MESH 2			
	λ_c^2		λ_a		λ_c^2		λ_a	
	CPU	loop	CPU	loop	CPU	loop	CPU	loop
<i>MS-RM</i>	7.68	81(23)	9.75	99(26)	23.22	97(25)	27.55	108(27)
<i>MS-RM-K_e</i>	14.70	892(92)	25.0	1441(144)	32.00	800(84)	60.21	1409(145)
<i>SS-RM</i>	7.68	81(23)	20.14	184(47)	23.22	97(25)	63.40	230(52)
<i>SS-RM-K_e</i>	14.70	892(92)	55.60	1841(185)	32.00	800(84)	136.07	1915(194)
MOSEK	0.96	15	2.52	17	2.75	15	5.37	16
MOSEK QP	2.36	25	11.42	28	7.61	26	30.70	40

point algorithm to the static shakedown theorem and in its solution by means of dual decomposition methods.

Two decomposition procedures, called respectively *MS-RM* and *SS-RM* have been presented. The first scheme, that proves to be the more effective, corresponds to the mathematical programming formulation of that used in [3, 4]. With respect to the previous proposal it proves to be more efficient also due to the use of a reference load formulation that makes the problem less nonlinear. The multisurface return mapping process is performed avoiding any linearization of the elastic domain exploiting an efficient sequential quadratic programming method and an active set strategy, so improving both accuracy and performance. The *SS-RM* is based on a standard return mapping process but requires a greater number of iterations each of which is almost as expensive as in the *MS-RM* case. For both the decomposition methods the elastic stiffness matrix can be exploited to obtain global convergent algorithms and to reduce the computational cost for very large dimension problems.

The shakedown strain driven analysis is easy to implement in existing commercial software performing nonlinear incremental elasto-plastic analysis. The lower efficiency with respect to IPM methods is compensated by its more significant mechanical interpretation that allows the reuse of the kinematical part of the solution and by, nowadays, a greater generality and robustness due to its consolidated and extensive use in this context of analysis.

References

1. Zouain, N.: Shakedown and safety assessment. In: Encyclopedia of Computational Mechanics, vol. 2, pp. 291–334. Wiley, New York (2004)
2. Armero: Elastoplastic and viscoplastic deformations of solids and structures. In: Encyclopedia of Computational Mechanics, vol. 2. Wiley, New York (2004)
3. Casciaro, R., Garcea, G.: An iterative method for shakedown analysis. Comput. Methods Appl. Mech. Eng. **191**, 5761–5792 (2002)
4. Garcea, G., Armentano, G., Petrolo, S., Casciaro, R.: Finite element shakedown analysis of two-dimensional structures. Int. J. Numer. Methods Eng. **63**(8), 1174–1202 (2005)

5. Boyd, S.: Lecture Slides and Notes. Courses EE364a and EE364b, <http://www.stanford.edu/class/ee364b/lectures.html>
6. Nocedal, Wright, S.J.: Numerical Optimization. Springer, Philadelphia (1997)
7. Bertsekas: Nonlinear Programming. Athena Scientific, Nashua (2003)
8. Nemirovski, A., Todd, M.: Interior-point methods for optimization. *Acta Numer.* **17**, 191–234 (2008)
9. Wright, M.H.: The interior-point revolution in optimization: history, recent developments, and lasting consequences. *Bull. Am. Math. Soc.* **42**(1), 39–56 (2005)
10. Krabbenhoft, K., Lyamin, A.V., Sloan, S.W., Wriggers, P.: An interior-point algorithm for elastoplasticity. *Int. J. Numer. Methods Eng.* **69**(3), 592–626 (2007)
11. Krabbenhoft, K., Damkilde, L.: A general non-linear optimization algorithm for lower bound limit analysis. *Int. J. Numer. Methods Eng.* **56**(2), 165–184 (2003)
12. Pastor, F., Loute, E.: Solving limit analysis problems: an interior-point method. *Commun. Numer. Methods Eng.* **21**(11), 631–642 (2005)
13. Vu, D.K., Yan, A.M., Nguyen-Dang, H.: A primal–dual algorithm for shakedown analysis of structures. *Comput. Methods Appl. Mech. Eng.* **193**, 4663–4674 (2004)
14. Nguyen, A.D., Hachemi, A., Weichert, D.: Application of the interior-point method to shakedown analysis of pavements. *Int. J. Numer. Methods Eng.* **4**(75), 414–439 (2008)
15. Makrodimopoulos, A.: Computational formulation of shakedown analysis as a conic quadratic optimization problem. *Mech. Res. Commun.* **33**, 72–83 (2006)
16. Makrodimopoulos, A., Martin, C.M.: Lower: bound limit analysis of cohesive frictional materials using second-order cone programming. *Int. J. Numer. Methods Eng.* **66**(4), 604–634 (2006)
17. Makrodimopoulos, A., Martin, C.M.: Upper bound limit analysis using simplex strain elements and second-order cone programming. *Int. J. Numer. Anal. Methods Geomech.* **31**(6), 835–865 (2007)
18. Ha, C.D.: A generalization of the proximal point method. *SIAM J. Control Optim.* **28**(3), 503–512 (1990)
19. Kaneko, Y., Ha, C.D.: A decomposition procedure for large-scale optimum plastic design problems. *Int. J. Numer. Methods Eng.* **19**, 873–889 (1983)
20. Ponter, A.R.S., Martin, J.B.: Some extremal properties and energy theorems for inelastic materials and their relationship to the deformation theory of plasticity. *Int. J. Mech. Phys. Solids* **20**(5), 281–300 (1972)
21. Liu, G.R., Nguyen-Thoi, T., Nguyen-Xuan, H.b., Lam, K.Y.: A node-based smoothed finite element method (NS-FEM) for upper bound solutions to solid mechanics problems. *Comput. Struct.* **87**, 14–26 (2009)
22. Bilotta, A., Casciaro, R.: An high–performance element for the analysis of 2D elastoplastic continua. *Comput. Methods Appl. Mech. Eng.* **196**, 818–828 (2007)
23. Garcea, G., Trunfio, G.A., Casciaro, R.: Mixed formulation and locking in path following nonlinear analysis. *Comput. Methods Appl. Mech. Eng.* **165**(1–4), 247–272 (1998)
24. A.S.: The MOSEK Optimization Tools Version 3.2 (Revision 8). User’s Manual and Reference Available from January (2005). <http://www.mosek.com>
25. Goldfarb, D., Idnani, A.: A numerically stable dual method for solving strictly convex quadratic programs. *Math. Program.* **27**, 1–33 (1983)
26. Bathe, K.J.: Finite Element Procedures. Prentice-Hall, New York (1996)
27. Groß-Wedge, J.: On the numerical assessment of the safety factor of elastic-plastic structures under variable loading. *Int. J. Mech. Sci.* **39**(4), 417–433 (1997)
28. Zouanin, N., Borges, L., Silveira, J.L.: An algorithm for shakedown analysis with nonlinear yield function. *Comput. Methods Appl. Mech. Eng.* **191**, 2463–2481 (2002)
29. Stein, E., Zhang, G.: Shakedown with nonlinear strain–hardening including structural computation using finite element method. *Int. J. Plast.* **8**, 1–31 (1992)
30. Zhang, X., Liu, Y., Cen, Z.: Boundary element methods for lower bound limit and shakedown analysis. *Eng. Anal. Bound. Methods* **28**, 905–917 (2004)

Limit State of Materials and Structures

Direct Methods 2

de Saxcé, G.; Oueslati, A.; Charkaluk, E.; Tritsch, J.-B.

(Eds.)

2013, VIII, 220 p., Hardcover

ISBN: 978-94-007-5424-9